THE JOURNAL OF PHYSICAL CHEMISTRY B

ARTICLE

pubs.acs.org/JPCB

Surface Structure of Sodium Dodecyl Sulfate Surfactant and Oil at the Oil-in-Water Droplet Liquid/Liquid Interface: A Manifestation of a Nonequilibrium Surface State

Hilton B. de Aguiar,[†,‡] Matthew L. Strader,[†] Alex G. F. de Beer,[†] and Sylvie Roke*[,†,‡]

[†]Max-Planck-Institut fuer Metallforschung, Heisenbergstrasse 3, 70569 Stuttgart, Germany

[‡]Institute of Bioengineering, School of Engineering, École Polytechnique Fédérale de Lausanne (EPFL), 1015 Lausanne, Switzerland

ABSTRACT: We present sum frequency scattering spectra on kinetically stabilized emulsions consisting of nanoscopic oil droplets in water, stabilized with sodium dodecyl sulfate (SDS). We have measured the interfacial structure of the alkyl chains of the surfactant molecules, the alkyl chain of the oil molecules, the weakly dispersive D_2O response, and the interference between SDS and the oil. We find a big difference in chain conformation: SDS has many chain defects, whereas the oil has very few. Our spectra are interpreted to originate from a surface structure with oil molecules predominantly oriented parallel with respect to the plane of the interface. The SDS headgroup is surrounded by water molecules. The SDS alkyl tail is in a disordered state and partially in contact with water. Such a conformation of surfactant occupies a surface area of several hundreds of squared angstroms.

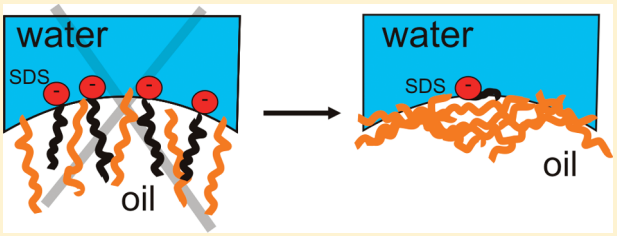

INTRODUCTION

If surfactants are added to an oil/water system, they will occupy the interfacial region until a significant portion of the surface layer is packed with surfactant. When the maximum coverage is reached, the surfactant will form micelles in the bulk phase. This concentration is called the critical micelle concentration.[1] This idea was proposed in the early 20th century[2,3] and originated from surface tension measurements that could be explained by a theory for oriented adsorption. Oriented adsorption in an oil/water system occurs with molecules that are amphiphilic, i.e., partially hydrophilic and partially hydrophobic. Such molecules have an affinity for both the oil and the water phase and are therefore highly surface active. The explanation for the lowering of surface tension was directly transferred to explain the experimental observation that emulsions appear to be stabilized by the same molecules that would reduce the surface tension.[4] From experiments on planar oil/water systems and microemulsions, it is widely accepted[1] that (i) in most cases a large amount of surfactant is needed to stabilize emulsions, that (ii) below the critical micelle concentration surfactants primarily reside as a somewhat oriented layer at the interface of the oil droplet in water, and (iii) that the hydrophobic tail will mix with the oil, while the hydrophilic headgroup will mix with the water.

In the past decades, this general picture has been refined by numerous experiments reviewed in, e.g., refs 5−7, involving X-ray diffraction,[7−13] neutron scattering,[9,14−22] (dynamic) surface tension measurements,[6,23−25] viscoelastic measurements,[26−29] second harmonic generation,[30] ellipsometry,[11,31−33] and sum frequency generation.[34−48] The anionic surfactant sodium dodecylsulfate (SDS) has been studied with sum frequency generation (SFG) at the air/water interface[34,38,42,43,47] and at the CCl_4/water interface.[35,37] Cationic alkyltrimethylammonium bromide surfactants have been studied with sum frequency generation (SFG) at the air/water interface[49−52] and the hexadecane/water interface.[40,46] Neutron reflection measurements have also been performed[22] as well as ellipsometry measurements of the temperature-dependent wetting of hexadecane.[33] These measurements have shown that three phases exist on this alkane/water/dodecyltrimethylammonium bromide (DTAB) interface: a 2D gas phase, a liquid phase comprising a mixed monolayer of hexadecane and the surfactant, and a 2D "solid" phase. Surfactants can also induce surface freezing,[31] which occurs on alkane/air interfaces[53] but, for reasons that are unclear, not on alkane/water interfaces.[9] Surfactant surface areas are reported in the range of 40−70 Å^2, whereby the occupied surface area is found to be larger on the oil/water interface than on the air/water interface.

The properties of kinetically stabilized emulsions are generally understood with the above-described behavior in mind.[54,55] Kinetic stability refers to the fact that, although the lifetime of an emulsion can be years, emulsions ultimately undergo a phase separation. Some observations can be interpreted as pointing toward a situation that requires a surfactant surface density that is much lower than 40−70 Å^2. For example, when droplet size in a kinetically stabilized emulsion is reduced down to the nanometer scale the droplet surface area becomes so large that the amount of surfactant in the sample is not enough to create interfaces with a

Received: January 18, 2011
Revised: February 7, 2011
Published: March 10, 2011

surfactant area of 40−70 Å^2. Instead, the calculated surface area is 10 to 100 times lower.[54] Nevertheless, nanoemulsions are very stable. It has also been reported[56−58] that stable emulsions can be prepared that do not require surfactant. The charge density needed to stabilize an emulsion is estimated to be in the range of 0.016 e$^-$/nm^2 (ref 59) to 0.3 e$^-$/nm^2 (ref 57). If this charge would originate from a surfactant, then it cannot be in correspondence with the mentioned surface area of 40−70 Å^2.

Commonly employed techniques for the study of fundamental processes that determine the structure and stability of kinetically stabilized emulsions typically probe parameters such as pressure or surface tension or overall charge (zeta potential),[57,61−63] which are not direct measures of the droplet interfacial molecular structure. For most molecular probes the surrounding medium forms an impenetrable barrier. As a result, the molecular interfacial properties of emulsion droplets are still unknown.[54,55,64]

Since the mid-90s pioneering work by the Eisenthal group has shown that Second Harmonic Scattering (SHS) could be used to elucidate the hidden properties of solid particles or droplets in solution.[65,66] Vibrational Sum Frequency Scattering[67,68] (SFS) spectroscopy builds upon those developments. It relies on the same principles as SHS with the additional feature that a vibrational spectrum can be recorded for any of the species that reside at the interface. In SFS experiments there are two important length scales: the molecular length scale of the molecules on the droplet interface and the size of the droplets. The latter is what makes scattering experiments distinctly different from reflection experiments from a planar interface (see ref 69 for a discussion of the differences). When droplets are in the size range of ∼100 nm they are large enough for the generated SF field to experience a different phase at different parts of the droplet surface. Thus, coherent addition of the generated SF photons on the droplet surface will lead to a nonvanishing SF signal that appears with a maximum scattering angle in a certain non-phasematched direction.

The molecular length scale is important as well. On the molecular length scale the local inversion symmetry determines whether an SF photon will be generated. An alkyl chain with an all-trans conformation and an even number of CH_2 groups has inversion symmetry centers between each interchain C−C bond. Selection rules dictate that there will be no SF photons emitted from the symmetric CH_2 stretch vibration (d^+ mode). In contrast, surface-bound all-trans chains are terminated by ordered CH_3 groups, so that coherent addition of the SF electric field components will result in a strong signal at the frequency of the symmetric CH_3 stretch vibration (r^+ mode). A collection of all-trans alkyl chains will therefore have an amplitude ratio of the d^+ mode and r^+ mode close to 0. If chain defects are present in the alkyl chains the inversion symmetry centers are removed, and the intensity of the symmetric CH_2 stretch vibration will increase. Coherent addition of the SF electric field components of a collection of randomly oriented methyl groups will result in a weak symmetric CH_3 stretch signal.[67,70,71] A collection of disordered alkyl chains will therefore have an amplitude ratio of the d^+ mode and r^+ mode that is large. The order in alkyl chains on a surface can therefore be represented by the d/r-ratio. This d/r-ratio has been determined for *n*-hexadecane at the hexadecane/air interface (at room temperature, 24 °C) where d/r = 3.3.[72] For SDS adsorbed on the water/CCl_4 interface in various amounts compared to the critical micelle concentration (cmc), the d/r-ratio ranges from d/r = 1.5 for SDS concentrations of 0.1 mM SDS down to d/r = 1−0.76, for SDS concentrations of 1−10 mM SDS.[35] The cmc of SDS is 8.1 mM at 298 K. For hexadecyltrimethylammonium bromide (CTAB) adsorbed on the *n*-hexadecane-d_{34}/D_2O planar interface values are reported ranging from d/r = 1.6 for CTAB concentrations of 0.05 mM down to d/r = 0.5, for CTAB concentrations of 0.6 mM. For CTAB adsorbed on the air/D_2O interface, values are reported ranging from d/r = 1.75 for CTAB concentrations of 0.05 mM down to d/r = 0.8 for CTAB concentrations of 0.9 mM at 298 K.[40] The cmc of CTAB is 0.9 mM.

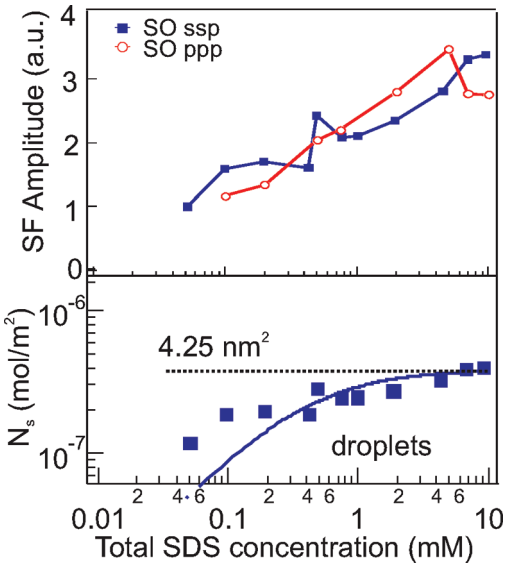

Figure 1. Top: SF amplitude in ssp and ppp polarization combinations of the sulfate stretch vibrational mode at 1070 cm^{-1}, obtained from measuring SF spectra of hexadecane droplets prepared with constant droplet size distribution and different total concentration of SDS surfactant. The SF amplitude is proportional to the SDS surface excess (N_s). Bottom: The corresponding upper limit for N_s, derived from the amplitude data. The solid blue line is a fit to the modified Langmuir adsorption model.

Recently, we have conducted SFS experiments on the oil droplet−water interface stabilized by SDS, in which we followed the change in surface density as a function of SDS concentration by monitoring the sulfate symmetric stretch scattered SF signal in multiple polarization combinations. For an emulsion series prepared with constant droplet concentration and size we found that the SF amplitudes change only by a factor of 3 when the total SDS concentration is varied from 50 μM to 10 mM. We concluded that the interfacial density of adsorbed SDS is at least 1 order of magnitude lower than the interfacial density at a corresponding planar interface. The derived maximum decrease in interfacial tension was only 5 mN/m.[73] The results of this study are summarized in Figure 1.

Here, we present SF scattering spectra on similar kinetically stabilized emulsions of sub-micron-sized oil droplets in water. Because we measure vibrational resonances, selective deuteration can be used to measure the interfacial structure of the alkyl chains of the surfactant SDS molecules, the alkyl chain of the oil molecules, the weakly dispersive nonresonant response, and the interference between SDS and the oil. We have determined the SDS alkyl chain conformation and the oil chain conformation, for different concentrations of SDS and different oil chain lengths. We find a big difference in chain conformation. SDS has many chain defects, and the oil has very few. Interference experiments and structure determination of SDS and oil as a

function of oil chain length are also described. We explain our observations using time scale arguments.

SFS BACKGROUND

In an SFS experiment, mid-infrared (IR) and visible (VIS) pulsed laser beams are overlapped inside a cuvette containing dispersed particles in a liquid or solid matrix.[74,75] At the droplet interface, a second-order nonlinear polarization ($\mathbf{P}^{(2)}$) is created which oscillates at the sum of IR and VIS frequencies. This polarization is small but does not vanish because there is a phase difference between the polarization components generated on different parts of the droplet surface. Therefore, sum frequency (SF) photons can be emitted. Interference of the SF field that is generated on different positions on the surface of the droplet produces a scattering pattern in the far-field. The scattering pattern depends on the droplet size[76−79] which, for the size range used in this study has, a broad maximum intensity at a scattering angle (θ) of $\theta \approx 60°$ as measured from the direction of the sum of IR and VIS wave vectors.

The SF intensity contains surface structural information and is resonantly enhanced when the energy of the IR photons equals the energy of a vibrational transition. Using a broad band femtosecond IR pulse, multiple vibrational resonances within a frequency range of ∼150 cm^{-1} are excited and subsequently upconverted by a narrow bandwidth VIS pulse. The resulting scattered spectrum represents the average vibrational spectrum of the interface of all droplets in the region where both laser pulses overlap.

To obtain the contribution of each vibrational mode, the spectra can be described with the following well-known expression, in complete analogy[68] with SFG experiments in reflection mode from planar interfaces[70]

$$I_{SFS}(\omega,\theta) \propto \left| \sum_n \left(A_{NR} f(\omega,\theta) e^{i\Delta\phi} + \frac{N_s A_n(\theta)}{(\omega - \omega_{0n}) + iY_n} \right) \right|^2 \quad (1)$$

where N_s is the surface density of molecular groups and A_{NR} is the amplitude of a weakly dispersive background, $f(\omega,\theta)$ the spectral shape of the weakly dispersive background, n a vibrational mode with resonance (RES) frequency ω_{0n}, $A_n(\theta)$ the angle-dependent amplitude, Y_n the half width at half-maximum of vibrational mode n, and $\Delta\phi$ the phase difference between the resonant and weakly dispersive background signal.

For the experiments described here, the spectral shape of the weakly dispersive background $f(\omega,\theta)$ can be measured by deuterating all components in the sample. For this case, the SF signal will be proportional to $|f(\omega,\theta)|^2$.

EXPERIMENTAL SECTION

Materials and Emulsion Preparation. The oil-in-water emulsions were made as follows: 2 vol % of oil (*n*-hexane, *n*-dodecane, or *n*-hexadecane) and a 1 mM solution of SDS (or d_{25}-SDS) in D_2O were mixed in a 4 mL vial using a hand-held homogenizer (TH, OMNI International) for 5 min. These mixtures were placed for 15 min in an ultrasonic bath (35 kHz, 400 W Bandelin), to produce emulsions that were stable against creaming. The resulting emulsion was used as a stock sample, which was further diluted with a solution of SDS in D_2O to obtain samples with a fixed volume fraction (1 vol %) and a varying final SDS concentration. The size distribution of the droplets in our samples was kept constant with a mean radius in the range of 80−130 nm and polydispersity index (PDI) of <0.2. For every data set, these values were determined by Dynamic Light Scattering (DLS), using a Malvern ZS nanosizer.

n-Hexadecane (C16), *n*-dodecane (C12), *n*-hexane (C6) (≥99%, Merck), d_{34}-hexadecane (*d*-C16), d_{26}-dodecane (*d*-C12) (98% D, Cambridge Isotope), D_2O (99% D, Aldrich), and d_{25}-SDS (*d*-SDS, 98% D, Cambridge Isotope) were used as received. Sodium dodecylsulfate (SDS) (>99%, Alfa Aesar) was purified by multiple recrystallization cycles in water and ethanol until the surface tension on water at a total concentration of 4 mM SDS (measured with a Wilhelmy plate method) was no longer changing (see ref 80). Glassware was cleaned with a 3:7 H_2O_2:H_2SO_4 solution, after which it was thoroughly rinsed with ultrapure water (0.053 μS/cm, TKA) to remove residual chemicals.

Laser System and Detection. The SF scattering experiments were performed using 1 kHz IR pulses centered around ∼2900 cm^{-1} (8−12 μJ, 150 fs, fwhm bandwidth 120 cm^{-1}) spatially and temporally overlapped with 800 nm VIS pulses (8−15 μJ, fwhm bandwidth 5−13 cm^{-1}) in a cuvette containing the emulsion. Detailed information about the laser setup can be found elsewhere.[81] IR and VIS pulses were focused down to a ∼0.4 mm beam waist under an angle of 15°. The polarization of the IR beam is controlled by two BaF_2 wire grid polarizers. The polarization of the VIS beam was controlled by a polarizer cube and a half-wave plate. p-Polarized beams are polarized parallel to the (horizontal) plane that contains all incoming and scattered beams, whereas s-polarized beams are polarized in the (vertical) plane perpendicular to that. Throughout the text, polarization combinations are defined with a three letter code with the SF polarization first and the IR polarization last. The cuvettes (Hellma 106 O.20-40) had a 0.2 mm optical path length and were made of detachable windows with the beam entrance side made out of CaF_2 and the beam exit side made out of quartz.

The SF scattered beam was collimated with a 0.5 in. diameter imaging lens (f = 18 mm, Thorlabs LA1074B) and directed toward the detection system with two 2 in. silver mirrors. The imaging lens was placed at a scattering angle (θ) of 60°, whereby the sample cell exit window was oriented perpendicular with respect to the outgoing scattered light. The SF signal was polarization selected with a Glan-Taylor CaF_2 prism and spectrally filtered with two short-pass spectral filters (Thorlabs FES750 and Omega Optical 3RD-770) placed before the entrance slit of the spectrometer (Shamrock 303i, Andor Technologies). The SF signal was spectrally dispersed onto an intensified CCD camera (i-Star DH742, Andor Technologies), which employed a timing gate of 8 ns. The acquisition time of a single spectrum was 300 s.

Recorded SF spectra are plotted as a function of IR wavenumber. The data were processed as follows: the data were baseline subtracted and normalized by dividing the measured counts by the input energies of the IR and VIS pulses (in microjoules, measured before the sample) and acquisition time (in seconds). This signal was divided by a normalized IR pulse spectrum, which is routinely measured before and after each experiment.

RESULTS

Surfactant vs Oil SF Spectra. To compare the structure of the surfactant alkyl and oil alkyl chains we have made use of selective deuteration of the surfactant, the oil, or both. Figure 2 shows SFS spectra of emulsions prepared with 8 mM h-SDS and d-C16

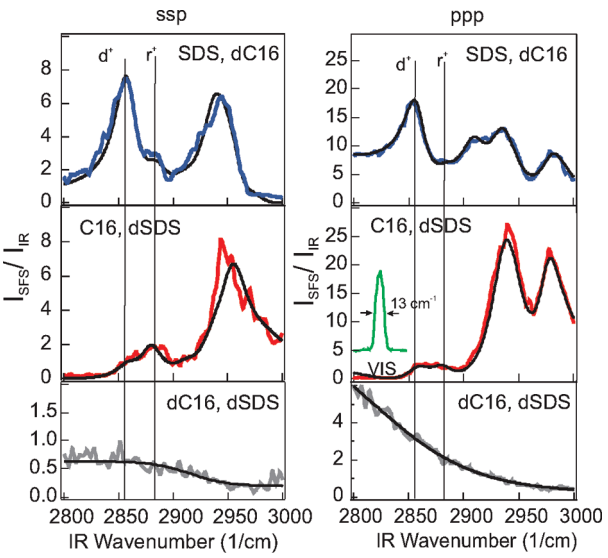

Figure 2. SFS spectra of the oil-in-water liquid/liquid interface of small droplets composed of 1 vol % *n*-hexadecane dispersed in D_2O and 8 mM SDS. Top: The h-SDS signal (using deuterated hexadecane). The droplets had an average radius of 103 nm. Middle: The h-C16 signal (using deuterated SDS). The droplets had an average radius of 103 nm. Bottom: the weakly dispersive nonresonant background, obtained using d-SDS and d-C16. The left (right) panel shows the ssp (ppp)-polarization. The black lines are fits as described in the text.

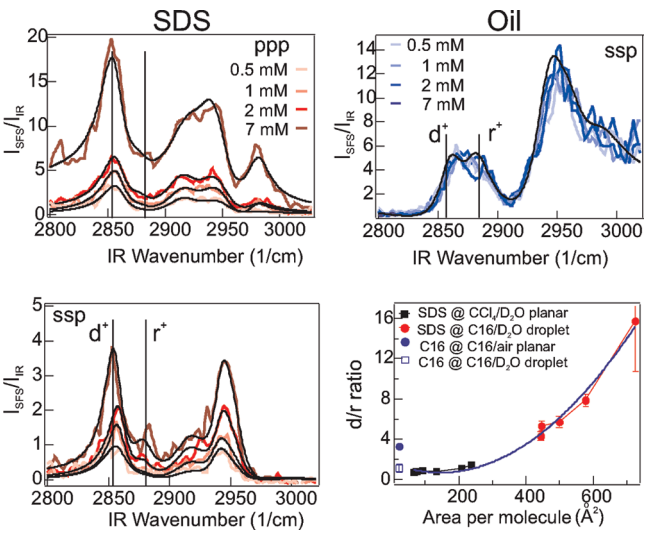

Figure 3. SFS spectra of the oil-in-water liquid/liquid interface of small droplets composed of 1 vol % *n*-hexadecane in D_2O and various amounts of SDS. Left panel: ppp-polarization (top) and ssp-polarization (bottom), for an emulsion made with SDS and fully deuterated oil, using 0.5, 1, 2, and 7 mM SDS (average radius = 120 nm). Right panel, top: SF spectra in ssp-polarization for an emulsion made with deuterated SDS at the same concentrations and nondeuterated *n*-hexadecane (average radius 130 nm). The top bottom panel shows a summary of d/r order parameters (red points) measured on the oil/water droplet interface for SDS surfactant and hexadecane oil, plotted against the surface area per molecule that was determined previously.[73] The black points for the SDS on the D_2O/CCl_4 planar interface were taken from ref 37, and the hexadecane/air interface was taken from ref 72. The solid line is a guide to the eye.

(top panel) or 8 mM d-SDS and h-C16 (middle panel) in D_2O. The left panels display polarization combination ssp, and the right panels display polarization combination ppp. From top to bottom the graphs show the signal of the SDS alkyl chains (using deuterated hexadecane, d-C16), the signal of the hexadecane alkane chains (using deuterated SDS, d-SDS), and the "nonresonant" or broadly dispersive background of the D_2O (using d-SDS and d-C16). The spectra were fit using eq 1, whereby the polynomial fit to the measured response of the fully deuterated samples was used as $f(\omega)$. For both hexadecane and SDS, the resonant part is composed of the well-known spectral features of the C−H stretch modes: The symmetric methylene stretch vibration (d^+, at 2855 cm^{-1}), the symmetric methyl stretch mode (r^+, at 2878 cm^{-1}), the Fermi resonance of the CH_3 bending mode overtone with the CH_3 stretch mode (r^{FR+}, at 2939 cm^{-1}), and the asymmetric methyl stretch mode (r^-, at 2959 cm^{-1}). These values correspond well with those reported for hexadecane at the air/hexadecane interface, the D_2O/CTAB/hexadecane interface,[46] and SDS at the CCl_4/water interface.[35,72] In these spectra there is also a clear peak at 2980 cm^{-1}, which is not present in the mentioned references.

If we divide the vibrational response of the d^+ mode by that of the r^+ mode we get d/r ratios that can be used to quantify the order in the alkyl chains (i.e., a measure of the number of non-all-trans bonds). For *n*-hexadecane we obtained, by averaging over 11 data sets, a d/r-ratio of 0.88 ± 0.42 and a phase difference $\Delta\phi$ between the weakly dispersive part and the resonance part of 0 ± 10°. In contrast, the spectrum of h-SDS has a peak at the symmetric CH_3 stretch mode with lower relative intensity, and the obtained d/r ratio is 4.3 ± 0.42 (determined by averaging over eight data sets). The obtained best fit for the phase difference $\Delta\phi$ between the weakly dispersive part and the resonances was 113° ± 10°. Both ppp and ssp data sets were fit with the same value of $\Delta\phi$, whereby we have used the weakly dispersive response that was measured for each polarization combination (displayed in the bottom part of Figure 2).

Effect of Surfactant Concentration. To get more insight into the large mismatch in d/r ratios (4.3 for h-SDS vs 0.88 for h-C16) we have taken SF spectra for emulsions prepared with changing bulk concentrations of SDS and followed the response of both the SDS (Figure 3, left panel) and the oil (Figure 3, right top panel). The left panel shows SFS spectra for different total concentrations of SDS, prepared with constant droplet density and total interfacial area. From 0.5 mM (0.06 × cmc) up to 8 mM (0.99 × cmc) the SF signal increases, which reflects an increase in SDS density at the interface. The change in intensity is a direct indication of a change in SDS interfacial density of a factor of ~2.6. The oil spectra are shown in the top right panel and show no change in intensity or spectral shape if the SDS concentration is increased.

For the SDS spectra the d/r ratios were determined in the same way as described above and varied from 4.2 up to 15 (from averaging over five data sets). The error bar at d/r = 15 indicates that the amplitude of the sym. CH_3 stretch mode has become so small that it is below the noise level. The d/r values for SDS are plotted in the bottom right panel of Figure 3. The surface areas per SDS molecule on the *x*-axis are upper limit values, determined from fitting the concentration-dependent SF response for various polarization combinations of the sulfate stretch mode to a modified Langmuir model using appropriate boundary conditions, as summarized in Figure 1. See ref 73 for a detailed description. Literature data for SDS on the D_2O/CCl_4 planar interface were taken from ref 37, and the values from the hexadecane/air interface were taken from ref 72.

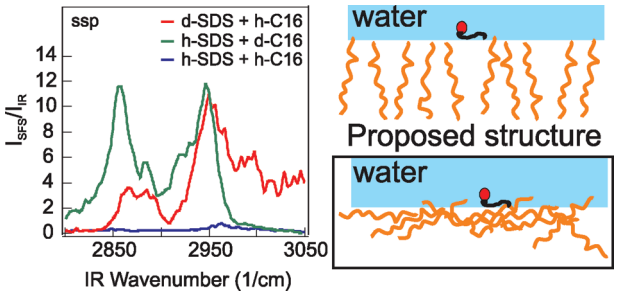

Figure 4. Left: Interference of SDS and C16. The green spectrum shows the ssp signal for droplets prepared with d-C16 oil and h-SDS. The red spectrum shows the ssp signal for droplets prepared with h-C16 oil and d-SDS. The blue spectrum shows the ssp signal for droplets prepared with h-C16 oil and h-SDS. Right: Illustration of possible surface scenarios. Top: The SF fields of one SDS molecule and one oil molecule cancel against each other. The majority of oil molecules determines the signal. This scenario does not explain the data. Bottom: The SF field of one SDS molecule has a comparable magnitude (but different phase) to the SF field generated by many oil molecules, resulting in near cancelation of the signal.

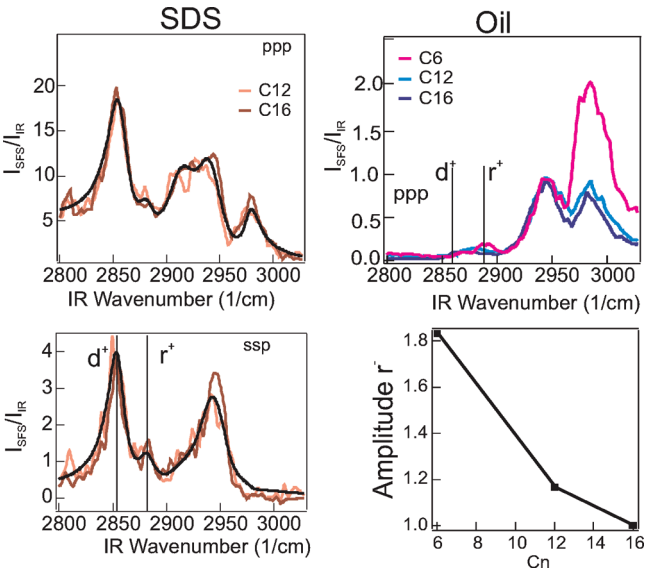

Figure 5. Left panel: SDS response as a function of oil chain length. SF scattering spectra of h-SDS on the oil-in-water liquid/liquid interface of droplets composed of either 1 vol % d-C16 in D_2O and 8 mM h-SDS (average radius = 95 nm) or 1 vol % d-C12 in D_2O and 8 mM h-SDS (average radius = 90 nm). Right panel top: Oil response as a function of oil chain length. SF spectra for emulsions composed of 1 vol % h-C16, h-C12, and h-C6 in D_2O prepared with 8 mM d-SDS. Right bottom panel: Amplitude of the asymmetric stretch mode for different alkane chain lengths.

Interference between the Oil and the SDS SF Response. To compare the signal strength of both the oil and the surfactant we have prepared emulsions with D_2O, hydrogenated oil (h-C16), and hydrogenated SDS (h-SDS) as constituents. Figure 4 shows the ssp spectra for three different samples: d-C16 + h-SDS, h-C16 + d-SDS, and h-C16 + h-SDS. It can be seen that the spectrum of the h-C16 + h-SDS sample has an extremely low intensity. This low intensity is caused by the interference of the electric field components of the C−H stretch modes of the oil and surfactant molecules on the interface. The phase difference between the oil and surfactant field causes destructive interference, which results in a nearly vanishing signal. Since the resultant field has almost vanished, the SF field from the SDS and the oil molecules is of nearly equal strength. The same result can be achieved starting from a surfactant-free emulsion, prepared with D_2O and h-C16. Adding h-SDS to the emulsion reduces the signal to the level observed in Figure 4.

Effect of Oil Alkyl Chain Length. To get more insight into the structure of the alkane layer and its interaction with the SDS at the interface, we have changed the oil alkane chain length and measured, again by selective deuteration, the response of both the SDS and the oil. The left panel of Figure 5 displays the h-SDS alkyl chain conformation in both ppp and ssp polarization, measured with d-C12 and d-C16 oil. It can be seen that when the oil chain length is decreased from d-C16 to d-C12 the SDS SF spectra are almost identical.

For the case of reversed deuteration, the SF signal for hexadecane (h-C16), dodecane (h-C12), and hexane (h-C6) droplets prepared with 8 mM d-SDS is plotted in the top left panel. It can be seen that the signal changes dramatically at the high frequency side when the chain length is decreased. The relative intensity of the asym. CH_3 mode increases significantly. The intensity of the sym. CH_3 mode increases as well, but this is less pronounced, as the r^+ and d^+ mode have a weak response in all h-alkane spectra. The bottom right panel displays the amplitude of the asym. CH_3 stretch mode, determined from spectral fitting.

DISCUSSION

Interpretation of the Data. Here, we will discuss the implications of the measurements done on the structure of the oil, the surfactants, and the interference measurements. Previously, we have conducted SFS experiments on the oil droplet/water interface stabilized by SDS, in which we followed the change in surfactant surface density as a function of SDS concentration. This was done by monitoring the sulfate symmetric stretch mode scattered SF signal in multiple polarization combination (see Figure 1 for a summary). It follows from eq 1 that the SF amplitude depends linearly on the surface density of vibrational groups. For an emulsion series prepared with constant droplet concentration and size, we found that the SF amplitude changes only by a factor of 3 when the total SDS concentration is varied from
50 μM to 10 mM. This allowed us to estimate that the *smallest* projected area per SDS molecule at the cmc was 4.25 nm^2 (this corresponds to a maximum surface density of $3.92 \pm 0.13 \times 10^{-7}$ mol/m^2).[73] We will describe our interpretation of the data, keeping the low surface densities in mind.

From the SF spectra in Figure 2, we have seen that the chain order in the alkane chains of the hexadecane is large so that the alkane chains that generate our spectra possess only a few gauche defects. The d/r-ratio of 0.88 ± 0.42 is smaller than the value reported by Esenturk et al. (d/r = 3.3, ref 72) for the hexadecane/air interface. This means that the hexadecane alkyl chains at the droplet oil/water interface are well ordered and a bit more ordered than hexadecane at the hexadecane/vapor interface. In contrast, the SDS at the interface (at 8 mM) has a d/r ratio of 4.3 which is indicative of a high number of gauche defects and a structure that is more disordered.

Clearly visible in the ppp spectra of SDS and C16 as well as in the ssp C16 spectrum is a peak at 2980 cm^{-1}, which has not been reported for either SDS on the CCl_4/water or hexadecane/air interface. It is most likely due to the asymmetric stretch mode of

the CH_3 groups. Further analysis on the exact assignment is needed, but it could be related to the interaction of CH_3 groups and water as suggested by Scheiner et al.[82]

Figure 3 (left panel) shows that if we increase the concentration of SDS (while keeping the droplet size distribution constant) the spectral intensity increases, which is indicative of an increased surface density. The SDS interfacial density is increased by a factor of ~2.6. This factor is in agreement with the data in Figure 1. Figure 3 (bottom right) shows the d/r values from our study plotted against the lower limit for the area per molecule as estimated earlier (see ref 73). The d/r values increase from 4.3 to 15, which means that the SDS becomes more disordered at lower concentrations and thus higher available surface areas. This is a consistent observation: a larger molecular area scales with a larger amount of conformational freedom. The d/r values reported for SDS at the planar CCl_4-D_2O interface[37] are plotted in the same figure. One can observe a trend in the molecular area vs d/r ratio curves that holds for both data sets: a more densely packed surface will have a more ordered conformation. The fit through the data points is a guide to the eye.

The oil spectra in Figure 3 (top right) show no change in intensity or spectral shape if the SDS concentration is increased. Thus, SDS does not strongly influence the oil SF response. This could be due to several effects:

(1) The SDS has such a low density that it perturbs only a tiny amount of the oil molecules. The signal change that results from SDS/oil interaction is below our detection limit.
(2) The SF signal originates from the second oil layer and not from the first.
(3) The SDS is not interacting strongly with the oil molecules.

The most likely of these three scenarios can be deduced by performing SFS experiments on a sample prepared with hydrogenated SDS (h-SDS) and hydrogenated oil (h-C16). Since the SF field components of oil and SDS are out of phase, there will be destructive interference between the electric SF field components generated from the oil and the SDS. If the SDS is at a too low concentration to perturb the oil signal (irrespective of orientation) or if we are measuring SF photons from the second oil layer only, the h-SDS + h-C16 spectrum will not be significantly different from the d-SDS + h-C16 spectrum. If, on the other hand, there is enough SDS on the surface to generate a signal comparable to the oil signal the h-SDS + h-C16 spectrum will be much lower in intensity than the d-SDS + h-C16 spectrum. Figure 4 shows that the h-SDS + h-C16 spectrum is much lower in intensity than the d-SDS + h-C16 spectrum. This indicates that there is enough SDS on the surface to interact with the oil. If the SDS would perturb the oil structure we would have to see a change in the oil spectra in the top right panel of Figure 3.

The question that now arises is: How can such a low density of surfactant have such a large effect in the interference experiment? On the oil/water surface the projected surface area of a perpendicular alkane molecule is ~22 Å^2. A parallel oriented molecule would have a larger projected area (up to ~80 Å^2). Thus, depending on the orientation, there are between 7 and 20 hexadecane molecules per SDS molecule on the droplet surface. The signal of one SDS molecule can compete with the signal of 7−20 oil molecules if there is a difference in orientation. Since the SF intensity is proportional to $N_s^2 <\cos \phi>^2$ (with N_s being the interfacial density, ϕ the angle between the C−C backbone and the surface normal, and <> the orientational average),[69] we need only a factor of $<\cos \varphi> \sim 0.05-0.14$ to explain the difference in signal. This can easily be achieved if the average orientational distribution of the oil would be such that the oil orients with an angle of ~81−85° with respect to the surface normal. It is important to note that, in contrast to reflection mode SFG experiments, for the SFS experiments presented here a change in molecular tilt angle will only influence the overall intensity and not the spectral shape of the signal. This is due to the size of the droplets and choice of scattering angle (see ref 69 for an explanation of these effects).

In contrast to an oil molecule oriented perpendicular with respect to the interface, a parallel oriented oil molecule would display a change in the methyl mode stretch intensity if the alkane chain length is varied (because the number of surface CH_3 groups changes). The result of changing the oil chain length on the oil SF signal can be seen in Figure 5. It shows that the spectral shape is preserved, with the most pronounced difference being a changing amplitude of the asym. CH_3 stretch mode. If the chain length is reduced from C16 to C6, the relative amplitude increases from 1 to 1.9. This would happen only if the oil molecules are oriented away from the surface normal.

Structure of the SDS Stabilized Oil/Water Interface. Considering all the experimental data, we arrive at a surface structure where the oil molecules are on average oriented more parallel than perpendicular to the surface plane. It is difficult to estimate the exact average orientation, but the observation of a change in the amplitude of the asym. CH_3 stretch mode is in agreement with a structure with oil molecules that are preferentially lying flat on the surface. The small d/r ratio indicates that oil molecules have a small number of chain defects. The blue shift observed in the asymmetric CH_3 stretch mode indicates that at least a portion of the CH_3 groups of the oil are in contact with the water. X-ray diffraction studies have shown that surface freezing is absent on the alkane/water interface,[9] while it occurs on the alkane/air interface.[31,53] This could be due to parallel oriented oil when it is in contact with water. Furthermore, theoretical simulations of the dodecane oil/water interface predict that "the dodecane molecules sitting at the first layer tend to lie flat".[83]

The SDS molecules have a low surface density and a large number of gauche defects. The sulfate headgroup consists of four O atoms that can act as hydrogen bond acceptors. Since hydrogen bonds are energetically more favorable than the van der Waals interactions between alkyl chains, it is likely that the headgroup is fully surrounded by water molecules and therefore adopts an orientation with its symmetry axis lined up on average with the surface normal. The oil is hydrophobic and nonpolar, and it is therefore reasonable to assume that there will be some distance between the O atom in the sequence S−O−C and the surface. The CH_2-CH_2 bond that follows will therefore be reasonably perpendicular. For the remainder of the SDS alkyl tail to be in contact with the oil, at least two chain defects are needed to bend the alkyl tail toward the surface. The blue shift observed in the asymmetric CH_3 stretch mode indicates that at least a portion of the CH_3 groups of the SDS are in contact with the water.

Summarizing our discussion, the SF data are consistent with oil molecules that are predominantly parallel oriented. SDS resides mainly on the water side, with its sulfate group interacting with water molecules. The alkyl tail can lie parallel on top of the oil only if it has chain defects. In such a structure, the CH_3 groups are partially exposed to water, which results in a blue shift of the asymmetric stretch mode. The bottom right panel of Figure 4 shows an illustration of this scenario. SDS molecules in such a

conformation can have projected surface areas of a few squared nanometers, if they are allowed to be free to rotate around the direction of the surface normal. This matches with our finding that the *smallest* projected area per SDS molecule at the cmc was 4.25 nm^2.[73]

Comparison to Planar Oil/Water Systems and Microemulsions. The number of experiments done on planar oil/surfactant/water systems and microemulsions is enormous (see, e.g., refs 5−22 and 30−48), and it is beyond the scope of our current work to treat them all here. There are however a few important differences between the experiments described here and measurements on planar systems and microemulsions:

(i) Microemulsions are thermodynamically stable but microscopically kinetically unstable mixtures of oil, water, surfactant(s), and/or salt. Kinetic instability here refers to the possibility that the droplet interfaces can merge so that new droplets can be formed, and exchange of contents between droplets is possible.[84] Typically, the interfacial tension is ultralow, and the droplets are small with diameters usually below 30 nm. The mixture can be characterized as a point in a phase diagram, and by changing the composition different mixtures and phases can be prepared. Microemulsions cannot be prepared with oil, water, and a single chained surfactant such as SDS[85] but need the presence of a cosurfactant, or a salt, or both, to be thermodynamically stable. A microemulsion can be considered as a solution of solubilized water or solubilized oil. An alternative name that has been suggested is "swollen micelles".[86] In contrast, the emulsions studied here are true emulsions: they are kinetically stable (i.e., no exchange is possible between the contents of the droplets on the time scale of the experiments) but thermodynamically metastable and consist of oil droplets surrounded by water.

(ii) Experiments on planar systems are often done on a water surface, which has been covered with surfactant. This layer is subsequently wetted by oil molecules. This gives a clear picture of solubilization of alkanes in surfactant layers (and it would be a comparable system to study the interactions in microemulsions). In our system, however, we have a pristine water/oil interface that interacts with surfactant. Such a neat interface can only with difficulty be prepared in a planar geometry (see, e.g., refs 9 and 40). In comparison, our sample contains several 100 cm^2 of interfacial area that is prepared in solution (without being exposed to air).

(iii) A planar oil/surfactant/water interface cannot spontaneously emulsify. It is therefore not necessarily comparable to the alkane/surfactant/water interfaces that we measure in our experiments, which is a kinetically stable, but ultimately thermodynamically metatable state.

(iv) Most surface specific measurements have not been performed with SDS, but with trimethylammonium (TA) salts (C_nTAB).[25,38,43] Besides being of opposite charge, there is a distinct difference in the chemical structure of the headgroups: the sulfate headgroup consists of oxygens that can hydrogen bond with the water, whereas the TA headgroup cannot form strong hydrogen bonds through the C−H groups. The interaction energy with water is therefore much larger for SDS (whereby electrostatic interaction and hydrogen bonding play a role) than for C_nTAB (whereby only electrostatic interaction will be the dominant driving force).

(v) Droplets experience Brownian motion and rotation, while a planar surface is static.

Explanation of Low Surface Coverage and Structure. We can offer a tentative explanation for the low density and structure of the interfacial layer by considering the time scales involved for making a surface and for the refreshment of the surface layer. The time scale needed to form a planar/static surface layer can be estimated from dynamic surface tension measurements. In a dynamic surface tension measurement, the surface tension is measured as a function of time by, e.g., analysis of the droplet shape of a newly formed hanging droplet. Dynamic surface tension measurements of aqueous SDS solutions against hexane show that the thermodynamic surface equilibrium state is reached in a time scale of seconds.[6,24,25] For a hanging droplet (with a size of a few millimeters) of an aqueous solution of 0.5 mM SDS that is newly formed in hexane, the hexane/water surface tension is reduced from its initial value of 51.1 to 48 mN/m in 0.01 s, to 38 mN/m in 0.1 s, and to its lowest value of 24 mN/m in a time scale of a few seconds. From this measurement we can conclude that the formation of a (static) surface that is in thermodynamic equilibrium with a solution that has a comparable bulk SDS concentration as in this study takes a few seconds.

The oil droplet interfaces in our emulsions undergo continuous changes due to droplet rotation and translation. The time scale of this movement can be estimated from the droplet diffusion time scale. From our DLS autocorrelation traces, we can deduce that on average the oil droplets have a mean square displacement of 200 nm in a time scale of 100 ms. In general (from Smoluchowski theory), a 100 nm droplet makes a complete rotation in 260 ms. Taking these numbers, on average it takes the droplet 0.72 ms to make a rotation of one degree, which corresponds to translation over a surface distance of 17 Å.

This crude estimate of time scales shows that the time scale needed to reach an interfacial equilibrium state is longer than the time scale at which the solution structure around the local surface is changing. It is therefore feasible that the interfacial layer cannot reach a thermodynamic equilibrium state. The equilibration of the surface structure is therefore not reached, and the surface structure is stuck at a state that is, under the nonequilibrium conditions, energetically and entropically the most favorable one.

Interestingly, Ichikawa et al.[87] have shown that application of a 10 kHz +20 V/−20 V square wave to a dense oil-in-water emulsion does not accelerate demulsification, whereas application of a 20 V/0 V square wave of the same frequency shortens the demulsification time from hours to only 1 min. The phenomenon was explained by the migration of (surface) charges that happens on the same time scale as the on/off switching of the kilohertz block pulse. This behavior is completely in line with our observations, as it implies that a surface charge reorganization happens on a time scale (0.1 ms) that is shorter than what is needed for the formation of an interfacial layer in thermodynamic equilibrium. It also offers an opportunity for additional study of the mechanism of surface formation.

■ CONCLUSIONS

In conclusion, the oil/water interface in a kinetically stabilized emulsion does not display the kind of structure that would be expected. The classical picture of emulsion stabilization requires that a large amount of surfactant is needed to stabilize emulsions and that below the critical micelle concentration a charged surfactant

forms an oriented monomolecular layer at the interface of the oil droplet in water, with the apolar tails interdigitated in the oil phase and the polar headgroup mixed with the water phase.

Vibrational sum frequency scattering spectra contain information about the molecular structure of the nanoscopic oil droplet−water interface. Because vibrational resonances are measured, selective deuteration can be used to measure the interfacial structure of the alkyl chains of the surfactant SDS molecules and the alkyl chain of the oil molecules. We have determined the SDS alkyl chain conformation and the oil chain conformation, for different concentrations of SDS and different oil chain lengths. We find a big difference in chain conformation. SDS has many chain defects, while the oil has very few. Interference experiments and structure determination of SDS and oil as a function of oil chain length are also described.

All data can be explained by a surface structure in which the oil is predominantly oriented parallel with respect to the interface. The SDS headgroup is surrounded by water molecules, and the alkyl tail needs a few chain defects to be in contact with the oil. Such a conformation of surfactant requires a surface area of several hundreds of squared angstroms. We can tentatively explain our observations by considering the interaction between oil and water and surfactant, whereby we take into account the time scales of Brownian motion and droplet rotation and compare it to the time scale on which an interface reaches its equilibrium state. Since the time scale needed to equilibrate a surface layer is longer than the time scale on which the interfacial structure changes (due to Brownian motion and droplet rotation) the surface state cannot reach equilibrium. The interface will therefore have a low density of surfactant.

AUTHOR INFORMATION

Corresponding Author

*E-mail: roke@mf.mpg.de, sylvie.roke@epfl.ch.

ACKNOWLEDGMENT

This work is part of the research programme of the Max-Planck Society. We thank the German Science Foundation (grant number 560398) and the European Research Council (Startup grant number 240556). M.L.S. acknowledges the Alexander von Humboldt Foundation.

REFERENCES

(1) Adamson, A. W.; Gast, A. P. *Physical chemistry of surfaces*; Wiley-interscience: New York, 1997.
(2) Langmuir, I. *J. Am. Chem. Soc.* **1917**, *39*, 1848–1906.
(3) Harkins, W. D.; Davies, E. C. H.; Clark, G. L. *J. Am. Chem. Soc.* **1917**, *39*, 354–364.
(4) Fischer, E. K.; Harkins, W. D. *J. Chem. Phys.* **1933**, *1*, 852–862.
(5) Bain, C. D. *Curr. Opin. Colloid Interface Sci.* **1998**, *3*, 287–292.
(6) Eastoe, J.; Rankin, A.; Wat, R.; Bain, C. *Int. Rev. Phys. Chem.* **2001**, *20*, 357–386.
(7) Schlossman, M. L.; Tikhonov, A. M. *Annu. Rev. Phys. Chem.* **2008**, *59*, 153–177.
(8) Tikhonov, A.; Mitrinovic, D.; Li, M.; Huang, Z.; Schlossman, M. *J. Phys. Chem. B* **2000**, *104*, 6336–6339.
(9) Schlossman, M. *Curr. Opin. Colloid Interface Sci.* **2002**, *7*, 235–243.
(10) Sloutskin, E.; Wu, X.; Peterson, T.; Gang, O.; Ocko, B.; Sirota, E. *Phys. Rev. E* **2003**, *68*, 031605.
(11) Sloutskin, Z., E.; Sapir; Bain, C. D.; Lei, Q.; Wilkinson, K. M.; Tamam, L.; Deutsch, M.; Ocko, B. M. *Phys. Rev. Lett.* **2007**, *99*, 136102−1–136102−4.
(12) Kashimoto, K.; Yoon, J.; Hou, B.; Chen, C.; Lin, B.; Aratono, M. *Phys. Rev. Lett.* **2008**, *101*, 076102.
(13) Mezger, M.; Sedlmeier, F.; Horinek, D.; Reichert, H.; Pontoni, D.; Dosch, H. *J. Am. Chem. Soc.* **2010**, *132*, 6735–6741.
(14) Cabane, B.; Duplessix, R.; Zemb, T. *J. Phys.* **1985**, *46*, 2161–2178.
(15) Chen, S. H. *Annu. Rev. Phys. Chem.* **1986**, *37*, 351–399.
(16) Lu, J. R.; Thomas, R. K.; Binks, B. P.; Fletcher, P. D. I.; Penfold, J. *J. Phys. Chem.* **1995**, *99*, 4113–4123.
(17) Eastoe, J.; Hetherington, K.; Sharpe, D.; Dong, J.; Heenan, R.; Steytler, D. *Langmuir* **1996**, *12*, 3876–3880.
(18) Hines, J.; Thomas, R.; Garrett, P.; Rennie, G.; Penfold, J. *J. Phys. Chem. B* **1998**, *102*, 9708–9713.
(19) Staples, E.; Penfold, J.; Tucker, I. *J. Phys. Chem. B* **2000**, *104*, 606–614.
(20) Thomas, R. K. *Annu. Rev. Phys. Chem.* **2004**, *55*, 391–426.
(21) Reynolds, P. A.; Henderson, M. J.; White, J. W. *Colloid Surf,. A* **2004**, *232*, 55–65.
(22) Zarbakhsh, A.; Webster, J.; Eames, J. *Langmuir* **2009**, *25*, 3953–3956.
(23) Aveyard, R.; Cooper, P.; Fletcher, P. *J. Chem. Soc., Faraday Trans.* **1990**, *86*, 3623–3629.
(24) Fainerman, V. *Colloids Surf.* **1992**, *62*, 333–347.
(25) Javadi, A.; Mucic, N.; Vollhardt, D.; Fainerman, V.; Miller, R. *J. Colloid Interface Sci.* **2010**, *351*, 537–541.
(26) Bonfillon, A.; Langevin, D. *Langmuir* **1993**, *9*, 2172–2177.
(27) Langevin, D. *Adv. Colloid Interface Sci.* **2000**, *88*, 209–222.
(28) Wilkin, J. N.; Mason, T. G. *Phys. Rev. E* **2007**, *75*, 041407−1–5.
(29) Georgieva, D.; Schmitt, V.; Leal-Calderon, F.; Langevin, D. *Langmuir* **2009**, *25*, 5565–5573.
(30) Conboy, J. C.; Daschbach, J. L.; Richmond, G. L. *Appl. Phys. A: Mater. Sci. Process.* **1994**, *59*, 623–629.
(31) Lei, Q.; Bain, C. D. *Phys. Rev. Lett.* **2004**, *92*, 176103−1–176103−4.
(32) Day, J.; Bain, C. D. *Phys. Rev. E* **2007**, *76*, 041601−1–041601−10.
(33) Matsubara, H.; Ohtomi, E.; Aratono, M.; Bain, C. D. *J. Phys. Chem. B* **2008**, *112*, 11664–11668.
(34) Ward, R. N.; Duffy, D. C.; Davies, P. B.; Bain, C. D. *J. Phys. Chem.* **1994**, *98*, 8536–8542.
(35) Messmer, M. C.; Conboy, J. C.; Richmond, G. L. *J. Am. Chem. Soc.* **1995**, *117*, 8039–8040.
(36) Conboy, J. C.; Messmer, M. C.; Richmond, G. L. *J. Phys. Chem.* **1996**, *100*, 7617–7622.
(37) Conboy, J. C.; Messmer, M. C.; Richmond, G. *Langmuir* **1998**, *14*, 6722–6727.
(38) Casson, B. D.; Bain, C. D. *J. Phys. Chem. B* **1998**, *102*, 7434–7441.
(39) Scatena, L. F.; Brown, M. G.; Richmond, G. L. *Science* **2001**, *292*, 908–912.
(40) Knock, M. M.; Bell, G. R.; Hill, E. K.; Turner, H. J.; Bain, C. D. *J. Phys. Chem. B* **2003**, *107*, 10801–10814.
(41) Brown, M.; Walker, D.; Raymond, E.; Richmond, G. *J. Phys. Chem. B* **2003**, *107*, 237–244.
(42) Hore, D.; Beaman, D.; Richmond, G. L. *J. Am. Chem. Soc.* **2005**, *127*, 9356–9357.
(43) Johnson, C. M.; Tyrode, E. *Phys. Chem. Chem. Phys.* **2005**, *7*, 2635–2641.
(44) Walker, D. S.; Moore, F. G.; Richmond, G. L. *J. Phys. Chem. C* **2007**, *111*, 6103–6112.
(45) Moore, F.; Richmond, G. L. *Acc. Chem. Res.* **2008**, *41*, 739–748.
(46) Wilkinson, K. M.; Qunfang, L.; Bain, C. D. *Soft Matter* **2006**, *2*, 66–76.
(47) Harper, K. L.; Allen, H. C. *Langmuir* **2007**, *23*, 8925–8931.
(48) McFearin, C.; Beaman, D.; Moore, F.; Richmond, G. *J. Phys. Chem. C* **2009**, *113*, 1171–1188.

(49) Bain, C. D.; Davies, P. B.; Ong, T. H.; Ward, R. N.; Brown, M. A. *Langmuir* **1991**, *7*, 1563–1566.
(50) Bell, G. R.; Bain, C. D.; Ward, R. N. *J. Chem. Soc., Faraday Trans.* **1996**, *92*, 515–523.
(51) Casson, B. D.; Bain, C. D. *J. Phys. Chem. B* **1999**, *103*, 4678–4686.
(52) Knock, M. M.; Bain, C. D. *Langmuir* **2000**, *16*, 2857–2865.
(53) Wu, X. Z.; Ocko, B. M.; Sirota, E. B.; Sinha, S. K.; Deutsch, M.; Cao, B. H.; Kim, M. W. *Science* **1993**, *261*, 1018–1021.
(54) Mason, T. G.; Wilking, J. N.; Meleson, K.; Chang, C. B.; Graves, S. M. *J. Phys.: Condens. Mater. Sci. Eng.* **2006**, *18*, R635–R666.
(55) McClements, J. D. *Crit. Rev. Food. Sci. Technol.* **2007**, *47*, 611–649.
(56) Aveyard, R.; Binks, B.; Clint, J. *Adv. Colloid Interface Sci.* **2003**, *100*, 503–546.
(57) Beattie, J. K.; Djerdjev, A. M. *Angew. Chem., Int. Ed.* **2004**, *43*, 3568–3571.
(58) Leunissen, M. E.; van Blaaderen, A.; Hollingsworth, A. D.; Sullivan, M. T.; Chaikin, P. M. *Proc. Natl. Acad. Sci.* **2007**, *104*, 2585–2590.
(59) Karraker, K. A.; Radke, C. J. *Adv. Colloid Interface Sci.* **2002**, *96*, 231–264.
(60) Beattie, J. K. *Chem. Phys. Lett.* **2009**, *481*, 17–18.
(61) Hunter, R. J. *Zeta potential in colloid science*; Academic Press: New York, 1981.
(62) Djerdjev, A. M.; Beattie, J. K. *Phys. Chem. Chem. Phys.* **2008**, *10*, 4843–4852.
(63) Creux, P.; Lachaise, J.; Graciaa, A.; Beattie, J.; Djerdjev, A. J. Phys. Chem. B **2009**, *113*, 14146–14150.
(64) Hunter, R. J. *Foundations of Colloid Science*; Oxford University Press: New York, 2002.
(65) Wang, H.; Yan, E. C. Y.; Borguet, E.; Eisenthal, K. B. *Chem. Phys. Lett.* **1996**, *259*, 15–20.
(66) Eisenthal, K. B. *Chem. Rev.* **2006**, *106*, 1462–1477.
(67) Roke, S.; Roeterdink, W. G.; Wijnhoven, J. E. G. J.; Petukhov, A. V.; Kleyn, A. W.; Bonn, M. *Phys. Rev. Lett.* **2003**, *91*, 258302.
(68) Roke, S. *Chem. Phys. Chem.* **2009**, *10*, 1380–1388.
(69) de Beer, A. G. F.; Roke, S. *J. Chem. Phys.* **2010**, *132*, 234702−1–8.
(70) Guyot-Sionnest, P.; Hunt, J. H.; Shen, Y. R. *Phys. Rev. Lett.* **1987**, *59*, 1597–1600.
(71) Gurau, M. C.; Castellana, E. T.; Albertorio, F.; Kataoka, S.; Lim, S. M.; Yang, R. D.; Cremer, P. S. *J. Am. Chem. Soc.* **2003**, *125*, 11166–11167.
(72) Esenturk, O.; Walker, R. A. *J. Chem. Phys.* **2006**, *125*, 174701−1–12.
(73) de Aguiar, H. B.; de Beer, A. G. F.; Strader, M. L.; Roke, S. *J. Am. Chem. Soc.* **2010**, *132*, 2122–2123.
(74) Roke, S.; Buitenhuis, J.; van Miltenburg, J. C.; Bonn, M.; van Blaaderen, A. *J. Phys.-Condens Matter* **2005**, *17*, S3469–S3479.
(75) de Beer, A. G. F.; de Aguiar, H. B.; Nijsen, J. W. F.; Roke, S. *Phys. Rev. Lett.* **2009**, *102*, 095502−1–4.
(76) Roke, S.; Bonn, M.; Petukhov, A. V. *Phys. Rev. B.* **2004**, *70*, 115106−1–10.
(77) Dadap, J. I.; de Aguiar, H. B.; Roke, S. *J. Chem. Phys.* **2009**, *130*, 214710−1–7.
(78) Jen, S. H.; Gonella, G.; Dai, H. L. *J. Phys. Chem. A* **2009**, *113*, 4758–4762.
(79) Jen, S.; Dai, H.; Gonella, G. *J. Phys. Chem. C* **2010**, *114*, 4302–4308.
(80) Lunkenheimer, K.; Pergande, H.-J.; Krueger, H. *Rev. Sci. Instrum.* **1987**, *58*, 2313–2318.
(81) Sugiharto, A. B.; Johnson, C. M.; de Aguiar, H. B.; Aloatti, L.; Roke, S. *Appl. Phys. B: Laser Opt.* **2008**, *91*, 315–318.
(82) Scheiner, S.; Grabowski, S.; Kar, T. *J. Phys. Chem. A* **2001**, *105*, 10607–10612.
(83) Bresme, F.; Chacon, E.; Tarazona, P.; Tay, K. *Phys. Rev. Lett.* **2008**, *101*, 056102−1–4.
(84) Eastoe, J. *Colloid Science, principles methods and applications*; Blackwell publishing: Cambridge, MA, 2005.
(85) Aveyard, R.; Binks, B. P.; Mead, J. *J. Chem. Soc., Faraday Trans. I* **1987**, *83* (8), 2347–2357.
(86) Friberg, S.; Mandell, L.; Larsson, M. *J. Colloid Interface Sci.* **1969**, *29*, 155–156.
(87) Ichikawa, T.; Dohda, T.; Nakajima, Y. *Colloids Surf., A* **2006**, *279*, 128–141.